United States
Environmental Protection
Agency

National Risk Management
Research Laboratory
Ada, OK 74820

Research and Development | EPA/600/SR-98/159 | July 1999

EPA

Project Summary

3DHYDROGEOCHEM:

A 3-Dimensional Model of Density-Dependent Subsurface Flow and Thermal Multispecies-Multicomponent HYDROGEOCHEMical Transport

Gour-Tsyh (George) Yeh and Hwai-Ping (Pearce) Cheng

A three-dimensional finite-element numerical model designed to simulate reactive chemical transport in subsurface systems with temperature effect taken into account is presented. The three-dimensional model is developed to provide (1) a tool of application, with which one is able to deal with a variety of real-world problems, (2) a tool of education, with which one can study how a factor would affect the whole system, and (3) a substructure, which one could modify to handle specific problems. The hydrological environment to which the model can be applied is a heterogeneous, anisotropic, saturated-unsaturated porous medium under either transient-state or steady-state flow conditions. In addition, the temperature within the system of interest can be both time- and location-dependent. For steady-state simulations, strong coupling among subsurface flow, reactive chemical transport, and heat transfer is used in the model. For transient-state simulations, weak coupling is used, but a density effect is still considered in computations. Both the strong and the weak couplings are pictured and explained in the original report. The model employs chemical equilibrium to describe the relationship among chemicals. The chemical reactions included in the model are aqueous complexation, multi-site adsorption/desorption, multi-site ion-exchange, precipitation/dissolution, redox, and acid-base reactions. To discretize the domain of interest appropriately, the element used in the model can be a hexahedral, a triangular prism, or a tetrahedral element. To extend its applicability to more real-world problems, two approaches are presented for the reactive chemical transport module. The first approach uses the pore velocity and dispersion coefficient to handle advection and dispersion, respectively, for aqueous components, whereas the second approach employs the retarded pore velocity and the retarded dispersion coefficient. Both approaches are designed to handle the problems with dominating precipitated species involved. In the original report, the governing equations of subsurface flow, reactive chemical transport, chemical equilibrium, and heat transfer are stated and/or derived, followed by the numerical strategies for solving the governing equations. In addition, twenty-five designed examples used to verify the model were described. Four application examples, including a three-dimensional subsurface flow example, a three-dimensional reactive chemical transport example, a three-dimensional heat transfer example, and a three-dimensional coupled flow-transport-transfer example, are presented to demonstrate the capability of the model.

The modeling experience from this study is summarized.

This Project Summary was developed by EPA's National Risk Management Research Laboratory's Subsurface Protection and Remediation Division, Ada, OK, to announce key findings of the research project that is fully documented in a separate report of the same title (see Project Report ordering information at back).

INTRODUCTION

3DHYDROGEOCHEM (a 3-Dimensional coupled model of HYDROlogic transport, GEOCHEMical equilibria, subsurface flow, and heat transfer in reactive multi-component/multi-species systems) has been developed mainly to study reactive chemical transport in subsurface systems. It is composed of two basic modules: flow and transport. In the flow module, the Galerkin finite element method is used to discretize the modified Richards' equation for simulating density-dependent subsurface flow. In the transport module, both reactive chemical transport and heat transfer are simulated. Their governing equations are discretized by using either the conventional Eulerian finite element method or the hybrid Lagrangian-Eulerian finite element method. In reactive chemical transport, solute transport is coupled with chemical equilibrium to consider the interaction among chemical species as they are transported by subsurface flow.

3DHYDROGEOCHEM has the following features which make it flexible and versatile in modeling a wide range of real-world problems: (1) Irregularly-shaped domains can be dealt with; (2) Both heterogeneous and anisotropic media, as many as desired, can be taken into account; (3) Both steady-state and transient-state simulations can be processed; (4) The initial conditions can be either prescribed or obtained by simulating a steady-state system under consideration; (5) Both distributed and point sources/sinks can be considered spatially- and/or temporally-dependent; (6) All types of boundary conditions can be considered spatially- and/or temporally-dependent; (7) The appropriate variable boundary conditions are determined automatically; (8) The "in-element" particle tracking technique is used to accurately and efficiently perform particle tracking; (9) Either the conventional Eulerian or the Lagrangian-Eulerian finite element method can be used to solve transport equations; (10) A numerical scheme of capturing peaks/valleys is employed to increase the computational accuracy of reactive chemical transport; (11) Multi-adsorbing site and/or multi-ion exchange site options are available to account for chemical reactions; (12) Many options are available to both compose and solve matrix equations, including (a) three options (under- , exact- and over-relaxation) to estimate the matrix in the strong coupling loop, (b) three options (under-, exact- and over-relaxation) to estimate the matrix in the nonlinear loops (i.e., the rainfall-evaporation loop in the subsurface module and the solute transport-chemical reaction coupling loop in the reactive chemical transport module), (c) four options (successive subregion block iteration, successive point iteration, polynomial preconditioned conjugate gradient, and incomplete Cholesky preconditioned conjugate gradient methods) to solve the linear/linearized matrix equations, (d) two options (consistent and lumping) to treat the mass matrix, (e) desired time weight factor, ranging from 0.0 to 1.0, to change the type of numerical scheme, and (f) two options, (the N+1 upstream or the Galerkin weighting functions) to compose the matrix equations when transport is simulated by the conventional Eulerian finite element method; (13) The time step size can be reset automatically when boundary conditions and/or sources/sinks change abruptly; (14) The examination of mass balance over the entire domain of interest for every time step is provided; (15) Many types of chemical reactions are included in 3DHYDROGEOCHEM, including aqueous complexation, adsorption/desorption, ion-exchange, precipitation/dissolution, redox, and acid-base reactions; (16) The extension of chemical reactions from chemical equilibrium to kinetics can be implemented without much difficulty in formulation. Table 1 briefly describes 3DHYDROGEOCHEM from another view.

DESCRIPTION OF THE MODEL

Mathematical Statements

3DHYDROGEOCHEM is designed to solve the following system of equations along with initial and boundary conditions, which describes water flow, heat transfer, and reactive chemical transport through saturated-unsaturated porous media.

The Governing Equation of Subsurface Flow

The governing equation for flow is basically the Richards' equation with density effect taken into account. Under the assumption of rigid media, the governing equation can be written as follows.

$$\frac{\rho}{\rho_o}\frac{d\theta}{dh}\frac{\partial h}{\partial t} = \nabla\left[K\left(\nabla h + \frac{\rho}{\rho_o}\nabla z\right)\right] + \frac{\rho^*}{\rho_o}q \qquad (1)$$

where h is the pressure head; t is time; ∇ is the divergence operator; **K** is the hydraulic conductivity tensor; z is the potential head; q is the source and/or sink; ρ is the groundwater density with dissolved chemical concentrations; ρ_o is the referenced groundwater density; ρ^* is the density of either the injected or the withdrawn groundwater; and θ is the moisture content. The hydraulic conductivity **K** is given by

Table 1. *The Property of 3DHYDROGEOCHEM*

Model Number	*18*
Model	*3DHYDROGEOCHEM*
Authors	*Cheng and Yeh*
Year	*1995*
Dimensions	*3*
Coupling Relation [a]	*F-H-C-T*
Coupling Method [b]	*Direct and 2-step*
Activity Coefficient [c]	*Davies*
Aqueous Complexation	*yes*
Sorption/Desorption [d]	*IE, SC, SL, and TL*
Precipitation/Dissolution	*yes*
Redox	*yes*
Temperature [e]	*V*

[a] *F-H-C-T denotes coupling among the flow equation, the heat transfer equation, the chemical relations, and the transport equations.*

[b] *Direct denotes strong coupling among the flow equation, the heat transfer equation, the chemical relations, and the transport equations; 2-step, weak coupling among flow, transfer, and transport but still strong coupling between the chemical relations and the transport equations.*

[c] *D-H denotes the extended Debye-Hückel equation.*

[d c] *IE denotes ion-exchange; SC, surface complexation; SL, single-layer model; and TL, triple-layer model.*

[e] *The temperature distribution can be either read in or computed.*

$$K = \frac{\rho g}{\mu} k = \frac{\left(\rho / \rho_o\right)\rho_o g}{\left(\mu / \mu_o\right)\mu_o} k_s k_r = \frac{\rho / \rho_o}{\mu / \mu_o} K_{so} k_r \quad (2)$$

where μ is the dynamic viscosity of the groundwater with dissolved chemical concentrations; ρ_o is the referenced groundwater dynamic viscosity; g is the gravity; $\mathbf{k}$ is the permeability tensor; $\mathbf{k}_s$ is the saturated permeability tensor; k_r is the relative permeability or relative hydraulic conductivity; and $\mathbf{K}_{so}$ is the referenced saturated hydraulic conductivity tensor. The referenced values are usually taken at zero dissolved chemical concentration. The Darcy flux is calculated as follows.

$$V = -K \cdot \left(\frac{\rho_o}{\rho} \nabla h + \nabla z \right) \quad (3)$$

To solve the governing flow equations in transient-state simulations, the pressure head over the domain of interest must be prescribed as the initial condition. This initial distribution of pressure head can be obtained by either field measurements or by solving the steady-state version of Equation (1). Four types of boundary conditions, from a mathematical point of view, are considered to deal with a variety of physical phenomena that can occur on the boundary. They are (1) prescribed total head (Dirichlet) boundary conditions which are used when the hydraulic head is known as a function of time on the boundary, (2) Neumann boundary conditions which are used when the groundwater flux due to the pressure head gradient is described as a function of time on the boundary, (3) Cauchy boundary conditions which are employed when the total groundwater flux, due to both the pressure and the potential head gradients, is described as a function of time on the boundary, and (4) Variable boundary conditions which are usually applied to the soil-air interface boundary (see the original report for full description).

The Governing Equations of Reactive Chemical Transport

Before the governing equations are described, the following nomenclature used in the model needs to be introduced:

$$\overline{T}_j = c_j + \sum_{i=1}^{M_x} a_{ij}^x x_i + \sum_{i=1}^{M_y} a_{ij}^y y_i + \sum_{i=1}^{M_z} a_{ij}^z z_i + \sum_{i=ndps+1}^{M_p} a_{ij}^p p_i \quad (4)$$

$$T_j = c_j + \sum_{i=1}^{M_x} a_{ij}^x x_i + \sum_{i=1}^{M_y} a_{ij}^y y_i + \sum_{i=1}^{M_z} a_{ij}^z z_i + \sum_{i=1}^{M_p} a_{ij}^p p_i \quad (5)$$

$$C_j = c_j + \sum_{i=1}^{M_x} a_{ij}^x x_i \quad (6)$$

$$S_j = \sum_{i=1}^{M_y} a_{ij}^y y_i + \sum_{i=1}^{M_z} a_{ij}^z z_i \quad (7)$$

$$P_j = \sum_{i=1}^{M_p} a_{ij}^p p_i \quad (8)$$

$$\overline{P}_j = \sum_{i=ndps+1}^{M_p} a_{ij}^p p_i \quad (9)$$

where $\mathbf{T}_j$ and $\overline{T}_j$ are the total analytical and modified total analytical concentrations of the j-th component, respectively; $\mathbf{C}_j$, $\mathbf{S}_j$, $\mathbf{P}_j$, and $\overline{P}_j$ are the total dissolved, total sorbed, total precipitated, and modified total precipitated concentrations of the j-th component, respectively; c_j is the concentration of the j-th component; x_i and a_{ij}^x are the i-th complexed species and its associated stoichiometric coefficient with respect to the j-th component, respectively; y_i and a_{ij}^y are the i-th adsorbed species and its associated stoichiometric coefficient with respect to the j-th component, respectively; z_i and a_{ij}^z are the i-th ion-exchanged species and its associated stoichiometric coefficient with respect to the j-th component, respectively; p_i and a_{ij}^p are the i-th precipitated species and its associated stoichiometric coefficient with respect to the j-th component, respectively; M_x, M_y, M_z, and M_p are the numbers of the complexed, adsorbed, ion-exchanged, and precipitated species, respectively; ndps is the number of the dominating precipitated species which are precipitated species with a concentration much higher than the total dissolved concentrations of their associated aqueous components. The aqueous components are mobile in subsurface systems, whereas the adsorbent components are immobile. The aqueous components may be involved in the complexation, adsorption/desorption, ion-exchange, and precipitation/dissolution reactions, whereas the adsorbent components can only be involved in the adsorption/desorption reaction. From another viewpoint, the aqueous components exist at least in the aqueous phase, whereas the adsorbent components exist only in the solid phase. The complexed, adsorbed, ion-exchanged, and precipitated species are the products of the complexation, adsorption, ion-exchange, and precipitation reactions, respectively.

The dominating precipitated species are arranged as the first ndps precipitated species so that they can be easily indexed in both derivation and formulation. To compute reactive chemical transport, three types of governing equations are basically solved: the governing equations of aqueous components, of adsorbent components, and of ion-exchange sites. Two approaches, defined as Approach 1 and Approach 2 in this report, are considered to deal with the reactive chemical transport of aqueous components.

For aqueous components:

< Approach 1 >

$$\theta \frac{\partial C_j}{\partial t} + \nabla \cdot \nabla C_j + \theta \frac{\partial \left(S_j + \overline{P}_j\right)}{\partial t} + \left(\theta \lambda_j + \frac{\partial \theta}{\partial t} + \frac{\rho^*}{\rho} q \right) \overline{T}_j - \nabla \cdot \left(\theta D \cdot \nabla \overline{T}_j\right) - \frac{\rho_o}{\rho} \overline{T}_j \nabla \left(\frac{\rho}{\rho_o} \right) \cdot \nabla = -\nabla \cdot \left[\theta D \cdot \nabla \left(S_j + \overline{P}_j\right)\right] + q C_j^* + \frac{\partial \theta}{\partial t} C_j + \frac{\rho^*}{\rho} q \left(S_j + \overline{P}_j\right) - \frac{\rho_o}{\rho} \left(S_j + \overline{P}_j\right) \nabla \left(\frac{\rho}{\rho_o} \right) \cdot \nabla - \sum_{i=1}^{ndps} a_{ij}^p \left[\frac{\partial (\theta p_i)}{\partial t} + \theta \iota_i^p \right] \qquad j \in [1, N_a] \quad (10)$$

< Approach 2 >

$$\theta \frac{\partial \overline{T}_j}{\partial t} + V \cdot \Lambda_{ij} \nabla \overline{T}_j + \left(\theta \lambda_j^a + \frac{\partial \theta}{\partial t} + \frac{\rho^*}{\rho} q \right) \overline{T}_j - \nabla \cdot \left(\theta D \cdot \Lambda_{ij} \nabla \overline{T}_j\right) - \frac{\rho_o}{\rho} \overline{T}_j \nabla \left(\frac{\rho}{\rho_o} \right) \cdot V = q C_j^* + \frac{\rho^*}{\rho} q \left(S_j + \overline{P}_j\right) - \sum_{i=1, i \neq j}^{NON} V \cdot \Lambda_{j,i} \nabla \overline{T}_i + \sum_{i=1, i \neq j}^{NON} \nabla \cdot \left(\theta D \cdot \Lambda_{j,i} \nabla \overline{T}_i\right) - \sum_{i=1}^{NSITE} V \cdot \Lambda_{j,NON+i} \nabla EC_i + \sum_{i=1}^{NSITE} \nabla \cdot \left(\theta D \cdot \Lambda_{j,NON+i} \nabla EC_i\right) - \frac{\rho_o}{\rho} \left(S_j + \overline{P}_j\right) \nabla \left(\frac{\rho}{\rho_o} \right) \cdot V + \frac{\partial \theta}{\partial t} C_j - \sum_{i=1}^{ndps} a_{ij}^p \left[\frac{\partial (\theta p_i)}{\partial t} + \theta \iota_i^p \right] \qquad j \in [1, N_a] \quad (11)$$

if

$$\left|\frac{\partial C_j}{\partial \overline{T}_j}\right| > \sum_{i=1, i\neq j}^{NON}\left|\frac{\partial C_j}{\partial \overline{T}_i}\right| + \sum_{i=1}^{NSITE}\left|\frac{\partial C_j}{\partial EC_i}\right| \tag{12}$$

For adsorbent components:

$$\theta\frac{\partial T_j}{\partial t} + \frac{\partial \theta}{\partial t}T_j = -\theta\lambda_j T_j \qquad j \in [N_a + 1, NON] \tag{13}$$

For ion-exchange sites:

$$\theta\frac{\partial EC_1}{\partial t} + \frac{\partial \theta}{\partial t}EC_i = -\theta\lambda_i^{EC}EC_i \qquad i \in [1, NSITE] \tag{14}$$

where θ is the water content; ι_i^p is the first-order decay rate of the i-th precipitated species; $\mathbf{EC}_i$ is the ion-exchange capacity of the i-th ion-exchange site; t is time; $\mathbf{V}$ is the Darcy flux; ∇ is the del operator; **D** is the dispersion coefficient tensor; λ_j and λ_i^{EC} are the decay constants of the j-th component and the i-th ion-exchange site, respectively; $\partial(\ )/\partial t$ is the partial derivative with respect to time; $\mathbf{C}_j^*$ is the total dissolved concentration of the j-th component in the source; $\mathbf{N}_a$ is the number of aqueous components; NON and NSITE are the numbers of components and ion-exchange sites, respectively; and $\Lambda_{j,j}$, $\Lambda_{j,i}$, and $\Lambda_{j,NON+j}$ are the concentration derivatives of $\partial C_j/\partial \overline{T}_j$, $\partial C_j/\partial \overline{T}_i$ ($1 \le \mathbf{i} \le \mathbf{NON}$), and $\partial C_j/\partial EC_i$ ($1 \le \mathbf{i} \le \mathbf{NSITE}$), respectively. The dispersion coefficient tensor **D** is given by:

$$\theta D = \alpha_T|V|\delta + (\alpha_L - \alpha_T)VV/|V| + \theta\alpha_m\tau\delta \tag{15}$$

where |**V**| is the magnitude of **V**; δ is the Kronecker delta tensor; α_T is transverse dispersivity; α_L is the longitudinal dispersivity; α_m is the molecular diffusion coefficient; and τ is the tortuosity. The first approach for aqueous components uses the pore velocities to both track particles in the Lagrangian step and compose matrix equations in the Eulerian step, whereas the second approach employs the retarded pore velocities to perform particle tracking as well as matrix composition. In both Equations (10) and (11), the dominating precipitated species is taken into account. If there is no dominating precipitated species existing in the system, the modified total precipitated concentration will be equal to the total precipitated concentration. In addition, the term showing the rate change of dominating precipitated species on the right-hand side of both equations no longer appears. In this case, the total analytical concentration, instead of the modified total analytical concentration, is the variable of interest to be solved for.

The whole set of governing equations of reactive chemical transport needs to be solved simultaneously because they are not a set of independent transport equations. In the model, all the chemical species in a system are related to one another under the consideration of chemical equilibrium. To solve for the concentration distributions of chemical species, the governing equations of reactive chemical transport are coupled with the governing equations of chemical equilibrium. They are solved iteratively until a convergent solution is reached. The governing equations of chemical equilibrium will be given below.

The initial condition used in transient-state simulations for reactive chemical transport includes the initial modified total analytical concentration of aqueous components, the initial concentration of dominating precipitated species; the initial total analytical concentration of the adsorbent components and ion-exchange sites. Four types of boundary conditions are employed for the simulation of reactive chemical transport. The boundary conditions are only required for aqueous (mobile) components because both adsorbent components and ion-exchange sites are considered immobile. Rather, the total analytical concentrations of adsorbent components and the ion-exchange capacities at a boundary node are computed in the same way as that of a node inside the domain. The four types of boundary conditions for aqueous components are (1) prescribed concentration (Dirichlet) boundary conditions which are used when the modified total analytical concentrations are known as functions of time on the boundary; (2) Variable boundary conditions which are applied when the flow direction varies with time during the simulation and the total dissolved concentrations in the incoming flow through the boundary are known as functions of time, (3) Cauchy boundary conditions which are used when the total fluxes, due to both advection and dispersion, are known as functions of time on the boundary, (4) Neumann boundary conditions which are employed when the dispersive fluxes are described as functions of time on the boundary.

The Governing Equation of Heat Transfer

The governing equation for heat transfer in a subsurface system can be derived based on the principles of conservation of energy and the law of thermal flux. By assuming (1) the thermal flux due to moisture gradient is small compared to that due to temperature and (2) the medium is rigid, the governing heat transfer equations can be written as follows.

$$(\rho C_l\theta + \rho_b C_m)\frac{\partial Temp}{\partial t} + C_l\rho V\cdot\nabla Temp - \nabla\cdot(\lambda I\cdot\nabla Temp) = S - \frac{\rho^*}{\rho}qC_l\rho Temp \tag{16}$$

where Temp represents temperature; $\boldsymbol{\rho}_b$ is the bulk density of the dry medium; $\mathbf{C}_l$ and $\mathbf{C}_m$ are the specific heats of groundwater and the dry medium in subsurface systems, respectively; λ is the apparent thermal conductivity; and **S** is the heat source. In using the results of solving Equation (16), the temperatures in both the solid and the liquid phases are thought as the same if they are both associated with the same representative elementary volume (REV) of a point of interest. The initial temperature distribution over the domain must be given for transient-state simulations. Four types of boundary conditions are included to simulate a variety of situations in practice. They are (1) Prescribed temperature (Dirichlet) boundary conditions which are used when temperature is known as a function of time on the boundary, (2) Neumann boundary conditions which are employed when the thermal flux due to conduction is described as a function of time on the boundary, (3) Cauchy boundary conditions which are utilized when the thermal flux due to both conduction and convection is given as a function of time on the boundary, and (4) Variable boundary conditions which are applied when the flow direction on the boundary may vary with time and when the temperature associated with the incoming flow is known as a function of time.

The Governing Equations of Chemical Equilibrium

The governing equations to determine chemical equilibrium, including the mole balance and mass reaction equations, are stated as follows.

Mole balance equations for aqueous components:

$$T_j = c_j + \sum_{i=1}^{M_x} a_{ij}^x x_i + \sum_{i=1}^{M_y} a_{ij}^y y_i + \sum_{i=1}^{M_z} a_{ij}^z z_i + \sum_{i=1}^{M_p} a_{ij}^p p_i \qquad j \in [1, N_a] \tag{17}$$

Mole balance equations for adsorbent components:

$$T_j = c_j + \sum_{i=1}^{M_y} a_{ij}^y y_i \qquad j \in [N_a + 1, N_a + N_s]$$

(18)

Mole balance equations for ion-exchange sites:

$$EC_i = \sum_{k-NOMZJ(i)+1}^{NOMZJ(i)+NOMZI(i)} \nu_k z_k \qquad i \in [1, NSITE]$$

(19)

Mass action equation for aqueous complexation:

$$A_i^x = K_i^x \prod_{j=1}^{N_a} X_j^{a_{ij}^x} \qquad i \in [1, M_x]$$

(20)

Mass action equation for adsorption/ desorption:

$$B_i^y = K_i^y \left(\prod_{j=1}^{N_a} X_j^{a_{ij}^y} \right) \left(\prod_{j=N_a+1}^{N_a+N_s} X_j^{a_{ij}^y} \right) \qquad i \in [1, M_y]$$

(21)

Mass action equation for ion-exchange reactions:

$$K_{k,LNI(i)} = \left(\frac{B_k}{A_k} \right)^{\nu_{LNI(i)}} \left(\frac{A_{LNI(i)}}{B_{LNI(i)}} \right)^{\nu_k}$$

(22)

Mass action equation for precipitation/ dissolution:

$$1 = K_i^p \prod_{j=1}^{N_a} X_j^{a_{ij}^p} \qquad i \in [1, M_p]$$

(23)

where N_s is the number of adsorbent components; υ_k is the valence of the k-th ion-exchanged species; **NOMZI(i)** is the number of ion-exchanged species involved in the i-th ion-exchange site; **NOMZJ(i)** is the number of ion-exchanged species involved in the 1-st through the (i-1)-th ion-exchange sites; A_i^x is the activity of the i-th complexed species; K_i^x is the equilibrium constant of the i-th complexed species; X_j is the activity of the j-th component species; B_i^y is the activity of the i-th adsorbed species of surface complexation; K_i^y is the equilibrium constant of the i-th adsorbed species; **LNI(i)** is the number of the ion-exchanged species, which is taken as the reference species for the i-th ion-exchange site, on the ion-exchanged species list; $K_{k,LNI(i)}$ is equilibrium constant of the k-th ion-exchanged species; K_i^p is the equilibrium constant of the i-th precipitated species.

When the dominating precipitated species exists in the system, we introduce the modified total analytical concentration, rather than the total analytical concentration, of components to be the primary dependent variable for the system of reactive chemical transport.

Numerical Strategies

The numerical strategies employed in 3DHYDROGEOCHEM include (1) strong coupling among flow, heat transfer, and reactive chemical transport modules for steady-state simulations to ensure accurate results, (2) weak coupling among flow, heat transfer, and reactive chemical transport modules for transient-state simulations to save computer time, (3) Galerkin finite element method to solve the governing equation of subsurface flow, (4) (n+1) upstream weighting finite element to solve the steady-state version and the Lagrangian-Eulerian finite element method to solve the transient-state version of the governing equations of both reactive chemical transport and heat transfer, and (5) Newton-Raphson method to solve the governing equations of chemical equilibrium. In solving the governing equations of reactive chemical transport, the two approaches employed in the model to solve for the transport of aqueous components are emphasized. The associated numerical strategies, under the considerations of peak/valley capturing as well as the existence of dominating precipitated species, are also described in the computation dealing with the transport of aqueous components. The details of all numerical strategies can be found in Chapter 3 of the original report.

Sample Problems

The 3DHYDROGEOCHEM model has been verified with twenty-five example problems, as stated in the original report. It also has been applied to solve four three-dimensional problems, including a subsurface flow problem, a heat transfer problem, a reactive chemical transport problem, and a coupled flow-transport-transfer problem. The coupled problem is described in the following.

Problem Description

This sample problem is used to demonstrate the coupling among subsurface flow, heat transfer, and reactive chemical transport. The required universal parameters for the associated simulation are listed in Table 2.

For computing the temperature-dependent groundwater density, the following equation is employed in this example problem.

$$\rho_w(T) = a_1 + a_2 T + a_3 T^2 + a_4 T^3$$

(24)

where $\rho_w(T)$ is the temperature-dependent pure water density associated with temperature **T;** a_1, a_2, a_3, and a_4 are temperature-density relationship parameters. One thing that should be noted is that the referenced groundwater density ρ_o (= 997.04882 g/dm^3) is associated with the referenced temperature T_o (= 298.3 ^{o}K). Two materials are included: material 1 for the upper half and material 2 for the lower half as pictured by Figure 1. Material parameters needed for the simulation are given in Table 3. In computing subsurface flow, the following three equations are employed to describe the soil properties.

$$\theta = \theta_{eff} \qquad if\ h \geq 0$$

$$\theta = \theta_{eff} - \left[1 - \frac{h_a - h}{h_a} \right] \left(\theta_{eff} - \theta_a \right) \qquad if\ h < 0$$

(25)

$$K = K_{sat} \qquad \text{if } h \geq 0$$

$$K = K_{sat} \left[\frac{h_a - h}{h_a} \right] \qquad \text{if } h < 0$$

(26)

Table 2. *Universal Parameters Needed for the Simulation of the Sample Problem*

Universal parameter	***Value***
Referenced groundwater density, ρ_o [g dm^{-3}]	*997.04882*
Referenced groundwater dynamic viscosity, μ_o [g dm^{-1} day^{-1}]	*7.9056×10^5*
Referenced temperature, T_o [^{o}K]	*298.3*
Specific heat of groundwater, C_l [dm^2 day^{-1} ^{o}K^{-1}]	*3.12035×10^{15}*
Density-temperature relationship parameter 1, a_1 [dimensionless]	*-410.174*
Density-temperature relationship parameter 2, a_2 [dimensionless]	*13.2296*
Density-temperature relationship parameter 3, a_3 [dimensionless]	*-0.0403921*
Density-temperature relationship parameter 4, a_4 [dimensionless]	*3.97476×10^{-5}*
Ideal gas constant, R [g dm^2 day^{-1} ^{o}K^{-1} mole^{-1}]	*6.2067×10^{15}*

$$\frac{d\theta}{dt} = \frac{\theta_a - \theta_{sat}}{h_a} \qquad (27)$$

The temperature-dependent equilibrium constant is calculated according to the van't Hoff equation. Table 4 lists chemistry information needed to compute chemical equilibrium for a simplified closed carbonate system that is considered in this application. The ionic-strength effect is taken into account by utilizing the extended Debye-Hückel formula.

Given well-designed pre-initial and boundary conditions, the steady-state simulation can provide a computational result that presents a uniformly-polluted domain under an isothermal and nearly hydrostatic condition. With this result as the initial condition, the temperature effect on a removal process can be investigated by activating a pumping well in the middle of the domain and controlling the flow-in groundwater with different temperatures. The detailed settings are described as follows. The pre-initial conditions are given 200 dm for the total head, 298.3 °K for the temperature, and 4×10^{-4} M for the total analytical concentrations of both Ca^{2+} and CO_3^{2-} throughout the entire domain. The pH-value is kept at 10. The top, bottom, front, and back boundaries are assumed impermeable for groundwater, heat, and chemicals to pass through. To perform the steady-state solution as mentioned above, a Dirichlet boundary condition of 200 dm is specified for the referenced total head on both the right and left boundaries while Variable boundary conditions are applied to those two boundaries for heat transfer and reactive chemical transport. The flow-in temperature is 298.3 °K. The flow-in concentration is 1.2247061×10^{-4} M for both Ca^{2+} and CO_3^{2-}, where 1.2247061×10^{-4} M is the total dissolved concentration for the two components at equilibrium when 4×10^{-4} M is the total analytical component concentration. Due to the density effect, a truly hydrostatic situation cannot be achieved. However, a nearly hydrostatic condition can be performed because the density effect is not important.

When the transient-state simulation begins, three point sinks are used to simulate a pumping well for a removal purpose. These three point sinks, with a pumping rate of 5×10^3 dm^3/day for each, are at (250, 100, 80), (250, 100, 90), and (250, 100, 95). It is thus imaginable that groundwater will flow into the domain through the left and the right boundaries. Relative clean groundwater, with a total dissolved concentration of 10^{-8} M for components 1 and 2, is assumed to supply

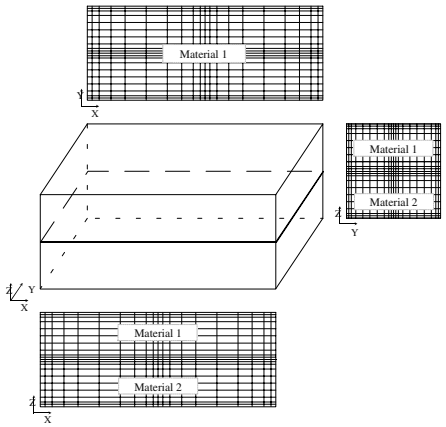

Figure 1. *The simulated domain of the sample problem.*

this flow-in groundwater. A temperature of 308.3 °K is associated with the flow-in groundwater through the left boundary, whereas the flow-in groundwater through the right boundary is still under the temperature of 298.3 °K. To put a focus on the temperature effect, the referenced total head of 200 dm is kept as in the steady-state simulation, so that the subsurface flow will be almost symmetric with respect to x = 250 dm (i.e., the middle of the domain in the x-direction). It is thus adequate, directly based on the computational results, to examine how significantly temperature can affect reactive chemical transport.

Forty time steps are included in the transient-state simulation, where 1, 2, and 4 days are set to be time-step sizes of the first, second, and third through fortieth time steps, respectively. 5×10^{-5} dm is assigned as the absolute error tolerance for a convergent solution of subsurface flow. In the meantime, 10^{-3} and 5×10^{-5} are used to be the relative error tolerances in computing for chemical concentrations and temperature, respectively.

Simulation Results

As mentioned above, the steady-state solution is controlled to be almost identical to the pre-initial condition. That is, the simulated domain has chemical concentrations uniformly distributed under an isothermal and a nearly hydrostatic condition at the beginning of the transient-state simulation.

With a pumping rate of 5×10^3 dm^3/day assigned to the three point sinks in the middle of the domain, a flow field, symmetric in the x-direction with respect to x = 100 dm,

Table 3. *Material Parameters Needed for the Simulation in the Sample Problem*

Material parameter	Material 1	Material 2
Saturated K_{xx} [dm day^{-1}]	*1.0*	*5.0*
Saturated K_{yy} [dm day^{-1}]	*1.0*	*5.0*
Saturated K_{zz} [dm day^{-1}]	*1.0*	*5.0*
Saturated K_{xy} (or K_{yx}) [dm day^{-1}]	*0.0*	*0.0*
Saturated K_{xz} (or K_{zx}) [dm day^{-1}]	*0.0*	*0.0*
Saturated K_{yz} (or K_{zy}) [dm day^{-1}]	*0.0*	*0.0*
Effective porosity, θ_{eff} [dimensionless]	*0.3*	*0.2*
Soil property parameter 1, θ_a [dimensionless]	*0.15*	*0.1*
Soil property parameter 2, h_a [dm]	*-1000.0*	*-1000.0*
Specific heat of dry medium, C_m [dm^2 day^{-1} °K^{-1}]	*1.0×10^{14}*	*2.0×10^{14}*
Apparent thermal conductivity, λ [g dm day^{-3} °K^{-1}]	*2.0×10^{18}*	*2.0×10^{18}*
Bulk density, ρ_b [g dm^{-3}]	*1200.0*	*1200.0*
Longitudinal dispersivity, α_L [dm]	*1.0*	*2.0*
Transverse dispersivity, α_T [dm]	*0.1*	*0.2*
Diffusion coefficient, α_m [dm^2 day^{-1}]	*0.0001*	*0.0002*
Tortuosity, τ [dimensionless]	*1.0*	*1.0*

Table 4. *Chemistry Data for the Simulation in Application 4*

Product species	Stoichiometric coefficient			Log_{10} K	Reaction enthalpy*
	Ca^{2+}	CO_3^{2-}	H^+		
OH^-	*0*	*0*	*-1*	*-14.000*	*4.167690×10^{19}*
HCO_3^-	*0*	*1*	*1*	*10.200*	*-1.112280×10^{19}*
H_2CO_3	*0*	*1*	*2*	*16.500*	*-1.171028×10^{20}*
$Ca(OH)_{2(s)}$	*1*	*0*	*-2*	*-21.900*	*1.256353×10^{19}*
$CaCO_{3(s)}$	*1*	*1*	*0*	*8.300*	*9.353595×10^{18}*

** The unit of reaction enthalpy is [g dm^2 day^{-2} mole^{-1}], 10 [kJ mole^{-1}] = 7.46496×10^{18} [g dm^2 day^{-2} mole^{-1}]*

can be observed when identical boundary conditions are applied to both the left and the right boundaries. In this application, however, a temperature of 308.3 °K is given to the incoming subsurface flow from the left boundary, which is 10 °K higher than that initially set for the simulated domain or that of the incoming subsurface flow from the right boundary. Thus, the groundwater density will not be symmetrically distributed in the x-direction. Based on the fact that the possible highest temperature is 308.3 °K and the possible maximum total analytical concentrations are 4×10^{-4} M for components 1 (i.e., Ca^{2+}), 2 (i.e., CO_3^{2-}) and less than 10^{-4} M for component 3 (i.e., H^+) through the whole simulation, the influence of temperature and chemical concentration on the groundwater density can be as large as 0.35% (according to Figure 4.24) and 0.004% (according to Eq. 2.35(b)) during the transient-state simulation.

Figures 2 and 3 present the total head distributions at time = 75 days and 155 days, respectively. The (a) part of these two figures puts a focus on planes y = 100 dm, y = 200 dm, and z = 100 dm, while part (b) concentrates on the planes of z = 50 dm, z = 100 dm, z = 150 dm, and y = 100 dm. A symmetry in the y-direction and an asymmetry in the z-direction can be seen as expected. Although the symmetry in the x-direction looks true, it does not exist actually due to the groundwater density effect mainly caused by a higher incoming temperature from the left boundary. Figure 4 plots the flow rate on both the left and the right boundaries at time = 75 days (part (a)) and 155 days (part (b)). Again, the magnitudes of the flow rates on the two boundaries cannot be distinguished visually. However, the computational result does provide values to tell the difference. On the other hand, since the groundwater density effect is so minor in this case that the difference mentioned above might be ignored, the subsurface flow could be assumed symmetric in the x-direction. The temperature-dependent removal process will be discussed later under this assumption.

Figure 5 shows the temperature distribution at time = 75 days with emphases on (a) plane z = 100 dm and (b) plane y = 100 dm. Likewise, Figure 6 plots the temperature distribution at time = 155 days. From Figure 5, only the isothermal line of 299 °K implicitly indicates a possible existence of pumping wells. The pumping, nevertheless, becomes obvious in Figure 6 because a longer simulation time allows heat to be transferred from the left boundary to the neighborhood of pumping wells, where the flow field is greatly dominated by pumping.

Figures 7 and 8 depict the computational results of simulating a removal process by pumping at time = 75 days and 155 days, respectively. In these two figures, part (a) is used to emphasize the total analytical concentration distribution on the planes of z = 65 dm and 135 dm, while part (b) is to describe the distribution of the total analytical concentration on planes y = 0 dm and y = 100 dm. Due to the fact that $Ca(OH)_{2(s)}$ does not exist under the competition with $CaCO_{3(s)}$ and dissolution is the only reaction of mass transfer between the solid and the aqueous phases through the transient-state simulation, the total analytical concentrations of component Ca^{2+}

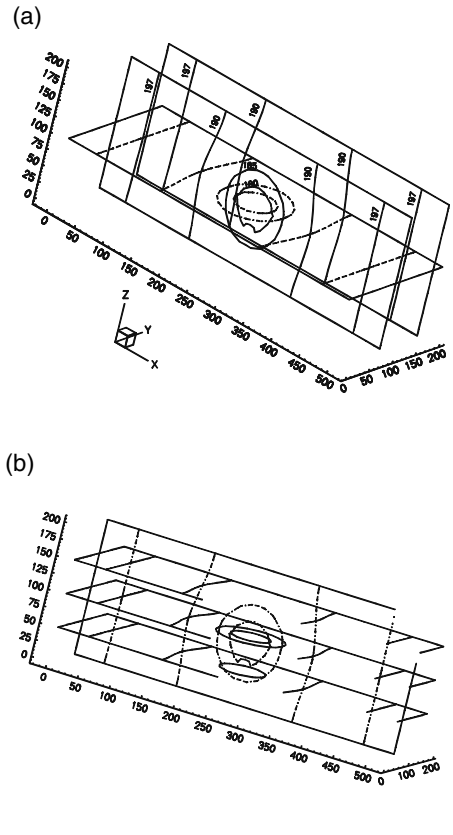

Figure 2. *The total head distribution at time = 75 days.*

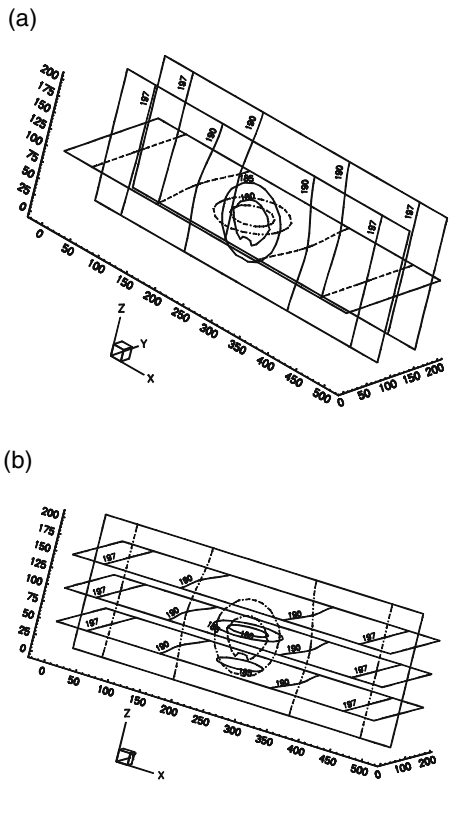

Figure 3*. The total head distribution at time = 155 days .*

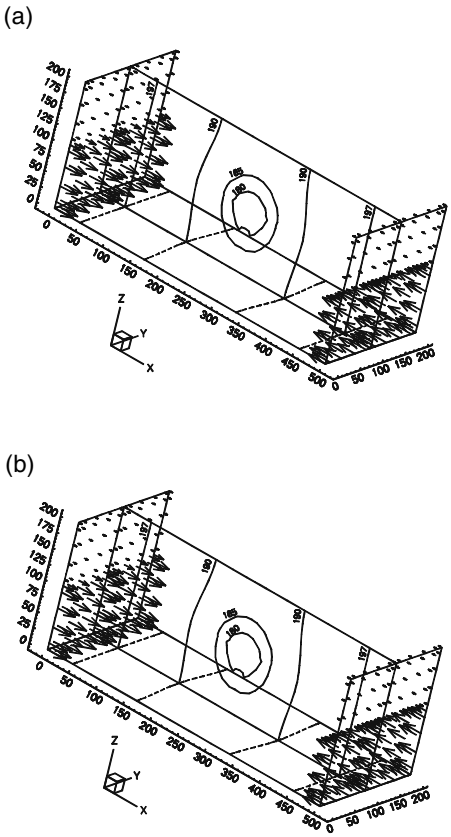

Figure 4*. The total head distribution and boundary flow rates at (a) time = 75 days and (b) time = 155 days.*

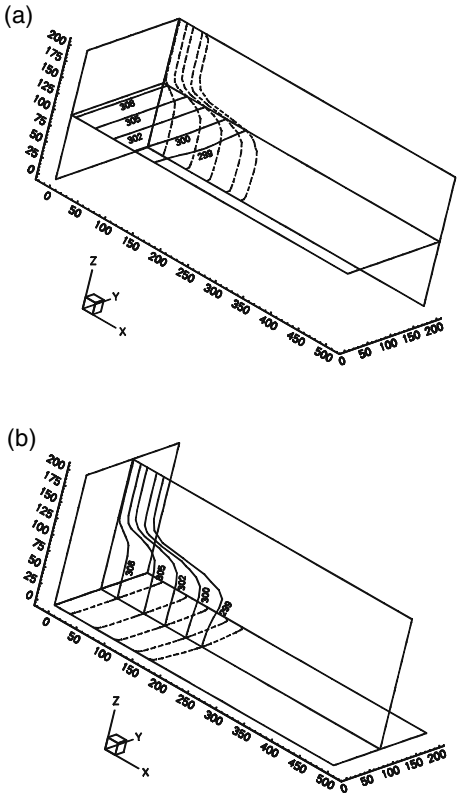

Figure 5. *The temperature distribution at time = 75 days.*

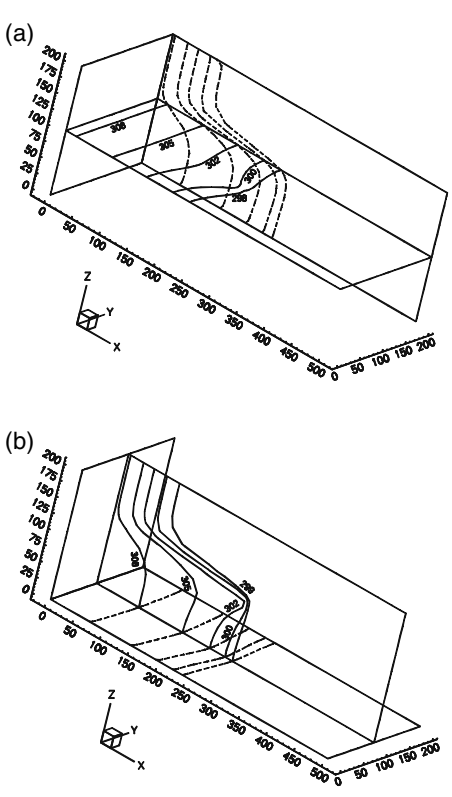

Figure 6. *The temperature distribution at time = 155 days.*

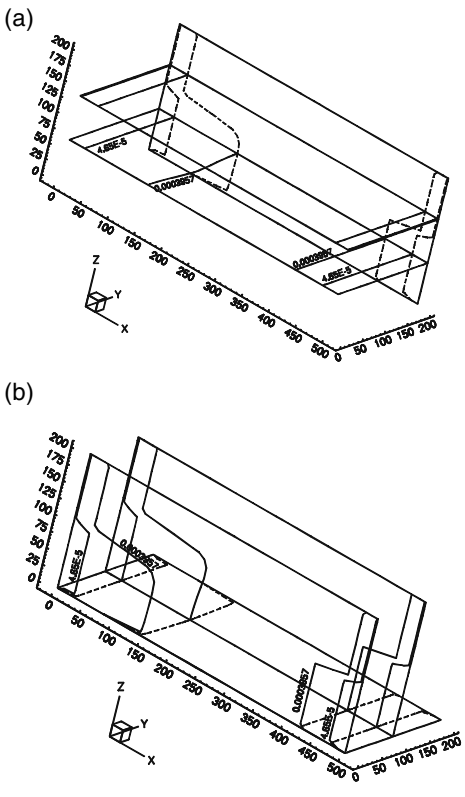

Figure 7. *The total analytical concentration distribution of component 1 (Ca^{2+}) or 2 (CO_3^{2}) at time = 75 days.*

and CO_3^{2-} are equal. This can be examined based on the prescribed equilibrium constants for such a simplified system. Therefore, the concentration distributions shown in Figures 7 and 8 can be for component Ca^{2+} or CO_3^{2-}.

Both figures point out that the higher incoming temperature from the left boundary drives the 0.0003957 M concentration line on the left side to move faster than that on the right side. But the $4.65x10^{-5}$ M concentration lines on both sides seem to move with the same progress toward the locations of sinks. As a matter of fact, the higher temperature makes this $4.65x10^{-5}$ M concentration line on the left move slower than that on the right. Figure 9 provides a two-dimensional concentration contour plot on the plane of y = 100 dm, which gives a clearer view on the two $4.65x10^{-5}$ M concentration lines at time = 155 days. The contrast between the 0.0003957 M and the $4.65x10^{-5}$ M concentration lines can be explained as follows.

According to the van't Hoff equation, a higher temperature will increase the equilibrium constant of a chemical reaction if the associated reaction enthalpy is positive. In this application, thus, a higher temperature coming in from the left boundary will help the precipitation of $CaCO_{3(s)}$ and increase the effort of completely removing the precipitant. This is why the $4.65x10^{-5}$ M concentration line on the left side migrates slower than that on the right side.

Given the total analytical component concentration, on the other hand, a higher temperature will cause a lower dissolved component concentration to be achieved at equilibrium. This lower dissolved component concentration at an upstream location and the current time will be brought to a downstream location along with the subsurface flow at the next time. Therefore, the total analytical component concentration at that downstream location will be reduced at the next time step if the temperature of the upstream location is higher than that of the downstream location at the current time. This basically explains what happens to the 0.0003957 M concentration line in this case. The faster moving concentration line on the left part of the domain causes less dissolved calcium (or carbonate) to migrate from upstream to downstream due to a higher upstream temperature.

The above discussion, in a way, implicitly signifies the need of numerical models for quantitative analyses: a higher temperature introduced from the upstream boundary will cause more precipitation of $CaCO_{3(s)}$ within the upstream region due to a positive reaction enthalpy, but it also generates a continuous dissolution within the downstream region due to the reduced total analytical concentration (as explained above) at a lower temperature. Under a lower temperature, a downstream location always has less total dissolved concentration coming in than going out, which makes this location undersaturated with the existence of precipitated species. To attain equilibrium, dissolution occurs to decrease the concentration of $CaCO_{3(s)}$ at this downstream location. These opposite situations hence lead to a difficulty in determining whether or not an introduction of a higher temperature from the upstream boundary would reduce the overall removal effort. To this point, a qualified numerical

(a)

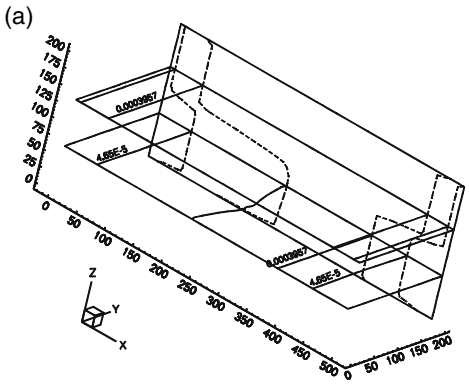

(b)

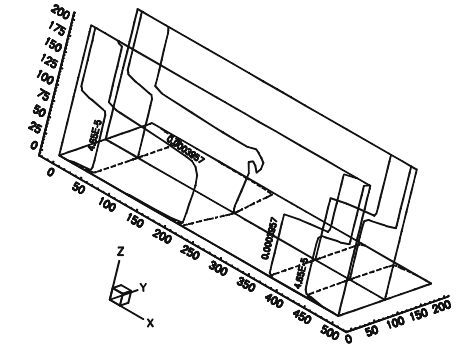

Figure 8. *The total analytical concentration distribution of component 1 (Ca^{2+}) or 2 (CO_3^{2-}) at time =155 days.*

model is required. One should be aware that the upstream and the downstream regions mentioned above are actually representing a relatively high-temperature and a relatively low-temperature region. Therefore, their sizes are to be changed with the transfer of heat. The speed of heat transfer, relative to that of reactive chemical transport, has been found able to significantly affect the removal result. This subject, even though not discussed here, could be interesting to environmental researchers and engineers.

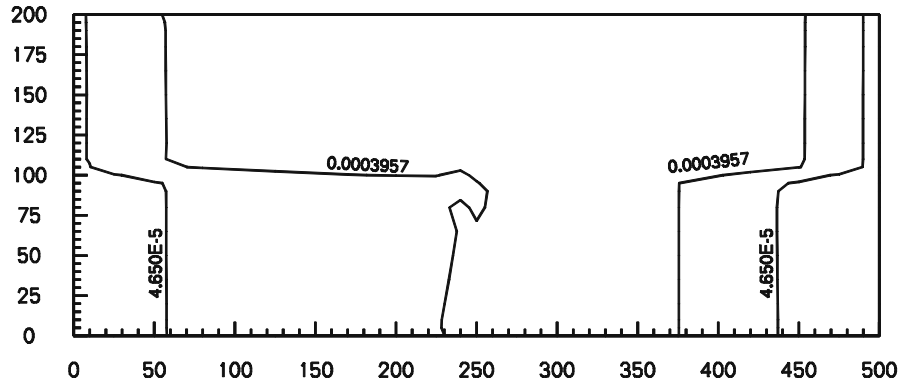

Figure 9. *The total analytical concentration distribution on the plane of y = 100 dm for component 1 or 2 at time = 155 days.*

Gour-Tsyh (George) Yeh and Hwai-Ping (Pearce) Cheng are with the Pennsylvania State University, University Park, CA 16802.
***Thomas E. Short** is the EPA Project Officer (see below).*
The complete report, entitled "3DHYDROGEOCHEM: A 3-Dimensional Model of Density-Dependent Subsurface Flow and Thermal Multispecies-Multicomponent HYDROGEOCHEMical Transport," (Order No. PB 99-150419; Cost: $41.00, subject to change) will be available only from:

National Technical Information Service
5285 Port Royal Road
Springfield, VA 22161
Telephone: 703-487-4650

The EPA Project Officer can be contacted at:

U.S. Environmental Protection Agency
National Risk Management Research Laboratory
Subsurface Protection and Remediation Division
P.O. Box 1198
Ada, OK 74820

United States
Environmental Protection Agency
Center for Environmental Research Information
Cincinnati, OH 45268

BULK RATE
POSTAGE & FEES PAID
EPA
PERMIT No. G-35

Official Business
Penalty for Private Use
$300

EPA/600/SR-98/159